

Accepted by ApJ Main Journal: 13 September, 2001

The new X-ray transient SAX J1711.6–3808: decoupling between its 3–20 keV luminosity and its state transitions

Rudy Wijnands^{1,2} & Jon M. Miller¹

ABSTRACT

We present a study of the correlated spectral and timing behavior of the new X-ray transient SAX J1711.6–3808 during its 2001 outburst using data obtained with the *Rossi X-ray Timing Explorer (RXTE)*. We also investigate the correlations between those source properties and the 3–20 keV X-ray luminosity. The behavior of the source during the observations can be divided into two distinct state types. During the “hard” state, the energy spectra are relatively hard and can be described by only a power-law component, and the characteristic frequencies (i.e., the frequency of the 1–7 Hz quasi-periodic oscillations observed for the first time in this source) in the power spectra are low. However, during the “soft” state, the spectra are considerably softer (in addition to the power-law component, a soft component below 8 keV is necessary to fit the spectra) and the frequencies are the highest observed. Remarkably, this distinction into two separate states cannot be extrapolated to also include the 3–20 keV X-ray luminosity. Except for one observation, this luminosity steadily decreased but the hard state was observed both at the highest *and* lowest observed luminosities. In contrast, the soft state occurred only at intermediate luminosities. This clearly demonstrates that the state behavior of SAX J1711.6–3808 is decoupled from its X-ray luminosity and that if the X-ray luminosity traces the mass accretion rate in SAX J1711.6–3808, then the state transitions are not good accretion rate indicators, or vice versa. The *RXTE* data of SAX J1711.6–3808 does not allow us to conclusively determine the exact nature of the compact object in this system. The source resembles both neutron star and black hole systems when they have low luminosities. We discuss our results with respect to the correlated timing and spectral behavior observed in other low-mass X-ray binaries and the implications of our results on the modeling of the outburst light curves of X-ray transients.

¹Center for Space Research, Massachusetts Institute of Technology, 77 Massachusetts Avenue, Cambridge, MA 02139-4307, USA; rudy@space.mit.edu; jmm@space.mit.edu

²Chandra Fellow

Subject headings: accretion, accretion disks — stars: individual (SAX J1711.6–3808) — X-rays: stars

1. Introduction

From simple accretion theory, one would expect that the X-ray luminosity in low-mass X-ray binaries (LMXBs) is directly related to the mass accretion rate³ (\dot{M}) in those systems. The X-ray spectra and the rapid X-ray variability of LMXBs most likely originate very close to the compact objects in those systems, in an environment which is dominated by changes in the mass accretion rate. Therefore, from this simple picture, the X-ray luminosity of LMXBs, their spectra, and their rapid variability should be directly related to \dot{M} and, thus, to each other. However, strong evidence is available that this scenario is an oversimplification of the behavior observed in LMXBs.

Especially for the persistent neutron-star LMXBs, it is well known that their timing behavior is very well correlated with their spectral behavior (as determined from the behavior in X-ray color-color diagrams), but much less well with the X-ray luminosity. This is also true for the transients systems for which enough data have been obtained to correlate the different parameters. For the neutron star systems, it is thought that the spectral and timing behavior are very well correlated with \dot{M} and that the X-ray luminosity is not. Due to an (as yet) unidentified process (or processes), a considerable fraction of the implied X-ray flux does not reach us (see van der Klis 1995, 2000 for detailed overviews and discussions about the neutron star LMXB behavior).

Until recently, the above described simple picture was thought to be an accurate description of the behavior of black-hole candidate (BHC) LMXBs, which could be described using the concept of source states (Tanaka & Lewin 1995; van der Klis 1995). In the BHC low-state (LS), \dot{M} is low, the energy spectra are hard, and the power spectra are dominated by a very strong (20%–50% rms amplitude) band-limited noise. In the high state (HS), \dot{M} is higher, the spectra are much softer, and in the power spectra only a weak (a few percent) power-law noise component is present. In the very high state (VHS), \dot{M} is the highest, the spectra are harder but not as hard as in the LS, and in the power spectra, noise is present similar to either the weak HS noise or the LS band-limited noise (although only with a strength of 1%–15% rms). Quasi-periodic oscillations (QPOs) near 6 Hz are detected, sometimes with a complex harmonic structure.

³When we discuss the mass accretion rate we implicitly assume the mass accretion rate through the disk and not through, e.g., radial inflow

However, it has become clear that the behavior of BHCs is far more complex than previously thought. First of all, QPOs are now observed not only during the hard VHS but also during hard states when the source luminosity is much less than during the VHS (e.g. the so-called intermediate states; Méndez & van der Klis 1997; Méndez, Belloni, & van der Klis 1998; Remillard et al. 1999b; Sobczak et al. 2000; Dieters et al. 2000; Homan et al. 2001a), but also a different type of QPO has been observed with frequencies up to 450 Hz (e.g., Remillard et al. 1999a,b; Homan, Wijnands, & van der Klis 2000; Cui et al. 2000; Homan et al. 2001a; Strohmayer 2001; Miller et al. 2001). However, the very detailed study of the new X-ray transient XTE J1550–564 performed by Homan et al. (2001a), using an extensive data set obtained with the proportional counter array (PCA) on board the *Rossi X-ray Timing Explorer (RXTE)* demonstrates best our lack of understanding of the behavior in BHCs. They showed that at least in this source (and possibly in more BHCs), the state behavior is completely decoupled from the X-ray luminosity and the state behavior of XTE J1550–564 must be described using two-dimensional diagrams. Besides the mass accretion rate, an unknown second parameter (e.g., the inner disk radius, the size of the Comptonizing region, the accretion flow geometry; Homan et al. 2001a) is involved in the formation of the states.

In this *Letter*, we discuss the correlated spectral and timing behavior of the new X-ray transient SAX J1711.6–3808 (in 't Zand, Kaptein, & Heise 2001) as observed with the *RXTE*/PCA, and the lack of correlation between its state transitions and the X-ray luminosity.

2. Observations and analysis

The new X-ray transient SAX J1711.6–3808 was discovered in February 2001 with the Wide Field Camera unit 1 on board *BeppoSAX* (in 't Zand et al. 2001). The source flux was between 30 and 80 mCrab (2–9 keV). The *RXTE* all sky monitor (ASM) light curve (not shown, but can be obtained from http://xte.mit.edu/ASM_lc.html) shows that the peak ASM count rate was between 4 and 5 counts s^{−1}, which corresponds to 50–70 mCrab (1.5–12 keV). Therefore, this source can be classified as a weak X-ray transient. During the first part of its outburst, proprietary *RXTE*/PCA observations were performed and are not yet publicly available. However, during the latter part of the outburst (i.e., the decay), several public TOO observations were performed which we used in our analysis (see Tab. 1 for a log of the observations). During these observations, data were taken simultaneously in the Standard 1 (1 energy channel and 1/8 s time resolution) and 2 modes (129 channels; 16 s resolution), and the event mode E_125US_64M_0_1S (64 channels; 122 μ s resolution). We

used the Standard 2 data to create a 2.9–18.8 keV count rate curve of the source and to create color curves. We used as soft color the count rate ratio between 4.1–7.5 keV and 2.9–4.1 keV, and as hard color the one between 11.4–18.8 keV and 7.5–11.4 keV.

Due to the different number of detectors (proportional counter units or PCUs) on during our observations, we only used data of the PCU 2, which was always on during our observations. PCU 0 was also continuously on during our observations, however this detector has lost its propane volume, which results in a higher background and occasional background flares. For weak sources like SAX J1711.6–3808, this would have considerable impact on the spectral results and, therefore, we have not included the data of this detector in our analysis. Although including only PCU 2 in our analysis gives limited results on an observation-by-observation basis, comparing the spectral results obtained with differing numbers of PCUs might introduce unwanted systematical effects. To obtain an homogeneous set of results, without extra systematic errors, we only use the data of PCU 2.

Routines from release 5.0.4 of the FTOOLS package were used to extract and reduce Standard 2 spectra from PCU 2 (data from all PCU layers were considered simultaneously). The tool “pcabackest” was used to extract background spectra, using the “bright source” model. Response matrices were generated using the tool “pcarsp.” Fits to PCA spectra of the Crab (a simple power-law at PCA resolution) often show significant residuals below 3.0 keV; for this reason we set 3.0 keV as a lower fitting limit. The source spectra become dominated by the background above 20 keV, so we adopt 20.0 keV as the upper limit to our fitting range. Power-law fits to the PCA spectra of the Crab show energy dependent residuals which can be as large as 1.0%. We therefore add 1.0% systematic errors to the spectra before fitting. The background-subtracted 3.0–20.0 keV X-ray spectra were analyzed using XSPEC version 11.01 (Arnaud & Dorman 2000). Errors on the fit parameters were calculated for the 90% confidence limits. The fluxes were obtained by measuring the flux at the best-fit values and the flux errors by measuring the flux at the 90% confidence limits for the given parameters (note that this method for obtaining flux errors will give the largest errors for those data sets which needed the most fit components; i.e. the third and fourth observations).

The absorption column was fixed to the Galactic column density towards this source (the weighted average obtained with the web-based tool nH is $1.4 \times 10^{22} \text{ cm}^{-2}$; Dickey & Lockman 1990⁴). However, for observation 60407-01-07-00 unacceptable fits were obtained

⁴nH can be found at <http://heasarc.gsfc.nasa.gov/cgi-bin/Tools/w3nh/w3nh.pl>; after submission of our paper, we learned that via an *XMM-Newton* observation of SAX J1711.6–3808 a column density was found which is consistent with what we used in our analysis (M. Santos-Lleo 2001 private communication)

when fixing the column density to this value. For this observation, the column density was a free parameter in the fits and we obtained a column of $4.2 \pm 0.5 \times 10^{22} \text{ cm}^{-2}$. The inclusion of extra components in fits (e.g., a soft component) to observation 60407-01-07-00 using the column density assumed for other observations did not allow for statistically acceptable fits. Similarly, using the column density obtained for observation 60407-01-07-00 in fits to the other observations did not yield significant statistical improvements, or allow the parameters of a soft flux component to be constrained in observations wherein a soft flux component is not indicated using the assumed column density (see below).

The X-ray spectra of LMXBs can be fit with a variety of models (e.g., Christian & Swank 1997). However, SAX J1711.6–3808 is a potential black-hole candidate and the X-ray spectra of those sources are usually fitted with a two-component model: a multi-color disk (MCD) black-body and a power-law. A similar amount of consensus is not present for the fit models for neutron star systems. Therefore, we did not concern ourself with other spectral models but only use the MCD plus power-law model for SAX J1711.6–3808. If this source contains a neutron star we might obtain unusual results via this model. By fitting the spectra with this model, a clear excess was apparent around 6–7 keV, which we fitted with a Gaussian with fixed centroid energy (6.4 keV) and width (1.2 keV). Although the equivalent width of this feature could be quite large (>0.5 keV), it is unclear what contribution is due to remaining calibration uncertainties of PCU 2 and/or due to the fit model assumed (note, that the strength and the variability of this feature might indicate that at least part of it is not due to remaining calibration uncertainties). A detailed investigation of this feature is beyond the scope of our paper, so we will not consider it further.

The event mode data (all data for all PCUs on) were used to create discrete FFTs using segments of 256-s data, resulting in power spectra for the frequency range 1/256–256 Hz. The power spectra were fitted with a broken power-law component to fit the band-limited noise, one or more Lorentzians for the broad bumps or QPOs, and a constant to account for the Poisson level. Errors on the fit parameters were calculated using $\Delta\chi^2=1$ and upper-limits were determined for $\Delta\chi^2=2.71$, corresponding to 90% confidence levels.

3. Results

The *RXTE*/PCA count rate curve (2.9–18.8 keV) is shown in Figure 1a and its corresponding 3.0–20.0 keV light curve in Figure 1b. A long term steady decreasing trend is apparent, although during observation seven (60407-01-07-00) the count rate and flux had slightly increased. The soft color (Fig. 1c) does not exhibit a similar smooth trend but it is clear that during the third and fourth observations (60407-01-03-00 and 60407-01-04-00),

the source spectra became considerably softer. During later observations the spectra were significantly harder again. The hard color (Fig. 1c) shows fewer but more erratic fluctuations, demonstrating that the softening of the spectra during observation three and four is mainly due to variations in the spectra at relatively low energies (<8 keV).

In Figure 2, several typical power spectra of SAX J1711.6–3808 are plotted. The power spectra of the source is dominated by a strong broad band-limited noise component, which can be modeled using a broken power-law with a break frequency (ν_{break}) of 0.2–2.0 Hz. Superimposed on this noise components, a broad bump or QPO is present with frequencies (ν_{QPO}) of 1–7 Hz. However, we note that the statistics of the data are not very constraining and other fit functions (e.g., only a set of Lorentzians) can be used to fit the data equally well. Also, the broad bump or QPO might have substructure due to sub-harmonics or overtones (note that only during observation three the first overtone could be detected at a $> 3\sigma$ level; see Tab. 1), however, the data do not allow to constrain this further. Only during observations three, four, and seven, the bumps on top of the band-limited noise can be considered true QPOs with Q values (frequency/FWHM) > 2 (Fig. 2b). This constitutes the first detections of QPOs for SAX J1711.6–3808.

The power spectra are very similar during the highest observed count rates (e.g., Fig. 2a, observation 60407-01-01-00) and lowest observed ones (e.g., Fig. 2c, 60407-01-05-00), with a ν_{break} and ν_{QPO} around 0.5 Hz and 1–2 Hz, respectively (see Tab. 1 for a detailed listing of the power spectral results). However, when the source was at intermediate count rates (e.g., during the third and fourth observations) the power spectra still had the same shape, but the characteristic frequencies had shifted to higher values (around 2 Hz and 7 Hz, respectively; Fig. 2b). These difference is also apparent in Figures 1d and 1f, which show ν_{break} and ν_{QPO} as a function of time. There is no apparent correlation between the count rate or flux and the properties of the broken power-law component and the QPO (i.e., their frequencies). But the frequencies of both components are well correlated with the soft color: the frequencies increase when the color decreases (compare, e.g., Fig. 1c with 1d). Such a correlation is not present between the frequencies and the hard color.

There is also a good correlation between the break frequency and the QPO frequency, which is exactly the correlation found for other LMXBs (Wijnands & van der Klis 1999), demonstrating that the rapid X-ray variability in SAX J1711.6–3808 is closely related to that seen in those other systems. For observation 60407-01-07-00, the QPO frequency seems to be higher than expected from this correlation; however, it is possible that only the first overtone of the QPO could be detected and not its fundamental (see also Wijnands & van der Klis 1999 for a general discussion of this effect on their correlation). This would put this observation exactly on the correlation. We searched for this possible fundamental but fitting

a Lorentzian with a fixed frequency at half the QPO frequency, did not reveal a significant detection (1.6σ detection for a FWHM of ~ 1 Hz) and a 95% confidence level upper limit on its strength is 6.7% rms. This limit is not very stringent and therefore we cannot exclude that indeed the detected QPO is the first overtone and not the fundamental. Despite these uncertainties, it is clear that the rapid variability of SAX J1711.6–3808 is very similar to what has been found for other LMXBs. Another correlation is that the strength of the band-limited noise and the QPO tend to decrease when the frequencies of those components increase. These correlations are not exact, but they are clearest for the QPO strength.

Typical energy spectra of SAX J1711.6–3808 are shown in Figure 3. In general, the spectra can be adequately fitted with a power-law model (but including a Gaussian component as explained above) with a power-law index of roughly ~ 2 (see Tab. 1 for a detailed overview of the spectral results). Including a multi-color disk black-body component in the fit, did not statistically improved the fit for most observations. However, during observation three and four, an extra soft component was necessary, which was fitted with a multi-color disk black-body model with a characteristic temperature of ~ 0.8 keV (see Tab. 1). In Figure 3, it can be clearly seen that observation four was considerably softer than observation one, with almost similar fluxes at the lowest energies but considerably lower fluxes at higher energies. The spectrum obtained during observation five was also considerably harder than the one for observation four, which is evident by the fact that both spectra cross each other at around 10 keV (Fig. 3). No apparent correlation is present between the power-law index and time or the count rate/fluxes, but a correlation is present between this parameter and the strength of the rapid X-ray variability. Both the strength of the broken-power law and the QPO tend to decrease when the power-law index increases.

4. Discussion

We report on the spectral and timing behavior of the new X-ray transient SAX J1711.6–3808 during the decay of its 2001 outburst. The rapid X-ray variability of SAX J1711.6–3808 can be consistently described by a broad band-limited noise component with a break frequency between 0.2 and 2 Hz. On top of this noise component a broad bump or a narrow QPO (only during observation three, four, and seven) is detected, whose frequency is strongly correlated with the break frequency. The frequencies of both components are not correlated with the X-ray luminosity, which, except for observation seven, decreases monotonically with time. The X-ray spectrum of the source is also not correlated with the luminosity but it is correlated with the timing properties. The spectrum is considerably softer (the inclusion of a soft component on top of the power-law is required) when the characteristic frequencies

in the power spectra are higher (observations three and four) compared with when they are significantly lower (the other observations). From our results, it is clear that during our third and fourth observations, the source was in a different, softer, state than during the other six observations. The occurrence of these states does not correlate with the X-ray luminosity. If the X-ray luminosity is a good indication of the mass accretion rate then the mass accretion rate monotonically decreased (except for observation seven) during the observations, but then the mass accretion rate is decoupled from the state transitions. However, it is also possible that still the mass accretion rate is coupled with the different states, but then the X-ray luminosity cannot be a good tracer of \dot{M} . In both scenarios it is difficult to explain why certain parameters in SAX J1711.6–3808 are coupled to the mass accretion rate but others are not.

In this respect, it is useful to consider that we only have the fluxes in a limited energy range (3–20 keV), which might not be an accurate indication for the total luminosity. A considerable amount of source flux could be hidden at luminosities above 20 keV. However, one crucial point can be made in this respect. During the first two of our observations, the source is the brightest in the 3–20 keV energy range and has relatively hard power-law spectra. However, during observation 3 and 4 the source is considerably dimmer and the spectra are much softer with steeper power-law tails. Therefore, no extra flux is expected to be present for those observations at higher energies (>20 keV, if extrapolating the spectral shape) which would make these observations brighter than the first two. This strongly suggest that the total X-ray flux during observation 3 and 4 was significantly lower than during observation 1 and 2. However, the spectra and the rapid X-ray variability of the source clearly demonstrate that the source had made a transit into a softer state, usually seen at higher luminosities. Therefore, the conclusion seems to be warranted that the X-ray luminosity is decoupled from the spectral and timing properties of the source.

SAX J1711.6–3808 is not the only source for which several source characteristics seem to be decoupled from the X-ray luminosity. As explained in the introduction, for the neutron star systems it is assumed that their correlated spectral-timing behavior is a good trace of the mass accretion rate and not the X-ray luminosity, mainly because of their correlations with other source parameters such as the emission at other wavelengths (optical, UV, line flux; Hasinger et al. 1990; Vrtilek et al. 1990, 1991; van Paradijs et al. 1990, Hertz et al. 1991; Augusteijn et al. 1992) and the X-ray burst properties (e.g., van der Klis et al. 1990; Munro et al. 2000; Franco 2001; van Straaten et al. 2001). However, Homan et al. (2001b) has pointed out that not all the behavior of the bright neutron-star LMXB GX 17+2 can be explained when assuming the above picture. Clearly, even for neutron star systems it is not completely settled how the different source properties depend on mass accretion rate. For BHs, this situation is even less well understood. Homan et al. (2001a) demonstrated that

the state behavior of the X-ray transient and BHC XTE J1550–564 was highly complex and completely decoupled from the luminosity, similar to what we observed for SAX J1711.6–3808 (although in much lesser degree than what was observed for XTE J1550–564, which could be due to the fewer observations and the lower luminosity of SAX J1711.6–3808). This demonstrates that BHCs can exhibit the same ambiguity as for the neutron-star systems with respect to how to trace \dot{M} .

At the moment, we cannot determine conclusively the nature of the compact object in SAX J1711.6–3808. Both the neutron star and the black hole systems have similar spectral and timing properties as we observe for SAX J1711.6–3808. If the source harbors a neutron star primary, then SAX J1711.6–3808 would most likely be of the atoll-type (see Hasinger & van der Klis 1989 for the neutron star classification) and the observed different states can then be identified with the island state (the hard states) and the lower banana branch (the soft state). However, the source might harbor a black hole. The spectral data of observation three and four required the inclusion of a soft component. The obtained MCD temperature of ~ 0.8 keV is typically what has been observed for BHCs, but still a neutron star primary cannot be excluded. If indeed a black-hole is present in SAX J1711.6–3808, then it would be the second BHC LMXB, after XTE J1550–564, for which it has been shown that the state transitions are not coupled to the luminosity of the source. The observed states can then be identified with the low state (the hard states) and the intermediate state (the soft state).

The main questions which remain are: (1) what causes this decoupling between the correlated spectral and timing behavior from the X-ray luminosity, and (2) which of the source properties traces \dot{M} best? The answer to the first question remains elusive. Moreover, both neutron-star and black-hole systems can exhibit this decoupling and it is even unclear if the same physical mechanism is responsible for this in both source types. The second question is also difficult to answer. Homan et al. (2001a) suggested that the states in the BHC XTE J1550–564 are decoupled from the mass accretion rate. However, if in this source and in the neutron star systems the same process is behind the decoupling of the states with luminosity, then it is possible that also for XTE J1550–564 the states are still coupled to \dot{M} but the luminosity is not, similar to the neutron star systems. The answers to the questions are especially important for the X-ray transients. If it can be proven that the X-ray luminosity is decoupled from \dot{M} , then this would have profound implications about our understanding of the outbursts observed for those transients. Usually, when those outburst light curves are modeled, it is implicitly assumed that the luminosity is a direct trace of \dot{M} . The results obtained from those models will lose their validity if this assumption turns out to be false. It is possible that even among systems with the same type of compact object, some light curves trace \dot{M} , while others do not. This may account (partly) for the different outburst light curve profiles observed for X-ray transients.

As a final point, we note that in the *RXTE*/PCA field of SAX J1711.6–3808 another X-ray transient is located, the X-ray burster SAX J1712.6–3739 (in 't Zand et al. 1999; Cocchi et al. 1999), which is about 0.5° from the position of SAX J1711.6–3808. One might worry about any possible contamination from this source to the X-ray flux we observe from SAX J1711.6–3808 and the possibility of this extra flux causing the decoupling we claim. We have no information about the X-ray state (quiescent or active) of SAX J1712.6–3739 at the time of our observations, and on first principle we cannot exclude any contribution of this source to the measured flux. However, as shown in Figure 1 *a* or *b*, during the first six observations the source declined steadily in count rate and flux. This behavior is expected for an X-ray transient which is decaying during its outburst. It would be very surprising if such a trend was produced by two independent sources, because they have to vary in X-ray luminosity in tandem. Also, the power spectra shown in Figure 2 are what is expected when only one source contributes to the X-ray flux. If multiple sources contributed, then the power spectra would be distorted because of the different timing properties of each source, unless by chance they would be very similar. We consider these options very unlikely and we conclude that the flux we observe is originating from SAX J1711.6–3808, and very likely suffers insignificant contamination from SAX J1712.6–3739.

This work was supported by NASA through Chandra Postdoctoral Fellowship grant number PF9-10010 awarded by CXC, which is operated by SAO for NASA under contract NAS8-39073. This research has made use of data obtained through the HEASARC Online Service, provided by the NASA/GSFC and results provided by the ASM/*RXTE* team. We would like to thank the referee, Keith Jahoda, for his very helpful comments. We also would like to thank him and Jean in 't Zand for pointing out the presence of the source SAX J1712.6–3739 in the *RXTE*/PCA field of view of SAX J1711.6–3808.

REFERENCES

- Arnaud, K. & Dorman, B. XSPEC v. 11.0
- Augusteijn, T., et al. 1992, A&A, 265, 177
- Christian, D. J. & Swank, J. H. 1997, ApJS, 109, 177
- Cocchi, M., Natalucci, L., in 't Zand, J., Heise, J., Muller, J. M., Celidonio, G., Di Ciolo, L. 1999, IAU Circ., 7247
- Cui, W., Shrader, C. R., Haswell, C. A., Hynes, R. I. 2000, ApJ, 535, L123
- Dickey, J. M. & Lockman, F. J. 1990 ARA&A, 28, 215

Dieters, S. W., Belloni, T., Kuulkers, E., Woods, P., Cui, W., Zhang, S. N., Chen, W., van der Klis, M., van Paradijs, J., Swank, J., Lewin, W. H. G., Kouveliotou, C. 2000, *ApJ*, 538, 307

Franco, L. M. 2001, *ApJ* in press (astro-ph/0009189)

Hasinger, G. & van der Klis, M., 1989, *A&A*, 225, 79

Hasinger, G., van der Klis, M., Ebisawa, K., Dotani, T., Mitsuda, K. 1990, *A&A*, 235, 131

Hertz, P., Vaughan, B., Wood, K. S., Norris, J. P., Mitsuda, K., Michelson, P. F., Dotanti, T. 1992, *ApJ*, 396, 201

Homan, J., Wijnands, R., & van der Klis, M. 2000, *IAU Circ.*, 7121

Homan, J., Wijnands, R., van der Klis, M., Belloni, T., van Paradijs, J., Klein-Wolt, M., Fender, R., Méndez, M. 2001a, *ApJS* 132, 377

Homan, J., van der Klis, M., Jonker, P. G., Wijnands, R., Kuulkers, E., Méndez, M., Lewin, W. H. G. 2001b, *ApJ* submitted (astro-ph/0104323)

in 't Zand, J., Heise, J., Bazzano, A., Cocchi, M., Smith, M. J. S. 1999, *IAU Circ.*, 7243

in 't Zand, J. J. M., Kaptein, R. G., & Heise, J. 2001, *IAU Circ.*, 7582

Méndez, M. & van der Klis, M. 1997, *ApJ*, 479, 926

Méndez, M., Belloni, T., & van der Klis, M. 1998, *ApJ*, 499, L187

Miller, J. M., Wijnands, R., Homan, J., Belloni, T., Pooley, D., Corbel, S., Kouveliotou, C., van der Klis, M., Lewin, W. H. G. 2001, *ApJ* letters, submitted (astro-ph/0105371)

Muno, M. P., Fox, D. W., Morgan, E. H., Bildsten, L. 2000, *ApJ*, 542, 1016

Remillard, R. A., McClintock, J. E., Sobczak, G. J., Bailyn, C. D., Orosz, J. A., Morgan, E. H., & Levine, A. M. 1999a, *ApJ*, 517, L127

Remillard, R. A., Morgan, E. H., McClintock, J. E., Bailyn, C. D., Orosz, J. A. 1999b, *ApJ*, 522, 397

Sobczak, G. J., McClintock, J. E., Remillard, R. A., Cui, W., Levine, A. M., Morgan, E. H., Orosz, J. A., Bailyn, C. D. 2000, *ApJ*, 531, 537

Strohmayer, T. E. 2001, *ApJ*, 522, L49

Tanaka, Y., & Lewin, W. H. G. 1995, In: *X-ray Binaries*, W. H. G. Lewin, J. van Paradijs, & E. P. J. van den Heuvel (eds.), Cambridge University Press, p. 126

van der Klis, M. 1995, In: *X-ray Binaries*, W. H. G. Lewin, J. van Paradijs, & E. P. J. van den Heuvel (eds.), Cambridge University Press, p. 252

van der Klis, M. 2000, *ARA&A*, 38, 717

van der Klis, M., Hasinger, G., Damen, E., Pennix, W., van Paradijs, J., Lewin, W. H. G. 1990, *ApJ*, 360, L19

van Paradijs, J., Allington-Smith, J., Callanan, P., Charles, P. A., Hassall, B. J. M., Machin, G., Mason, K. O., Naylor, T., Smale, A. P. 1990, *A&A*, 235, 156

van Straaten, S., van der Klis, M., Kuulkers, E., Méndez, M. 2001, *ApJ*, 551, 907

Vrtilek, S. D., Raymond, J. C., Garcia, M. R., Verbunt, F., Hasinger, G., Kurster, M. 1990, *A&A*, 235, 162

Vrtilek, S. D., Pennix, W., Raymond, J. C., Verbunt, F., Hertz, P., Wood, K., Lewin, W. H. G., Mitsuda, K. 1991, *ApJ*, 376, 278

Wijnands, R. & van der Klis, M. 1999, *ApJ*, 514, 939

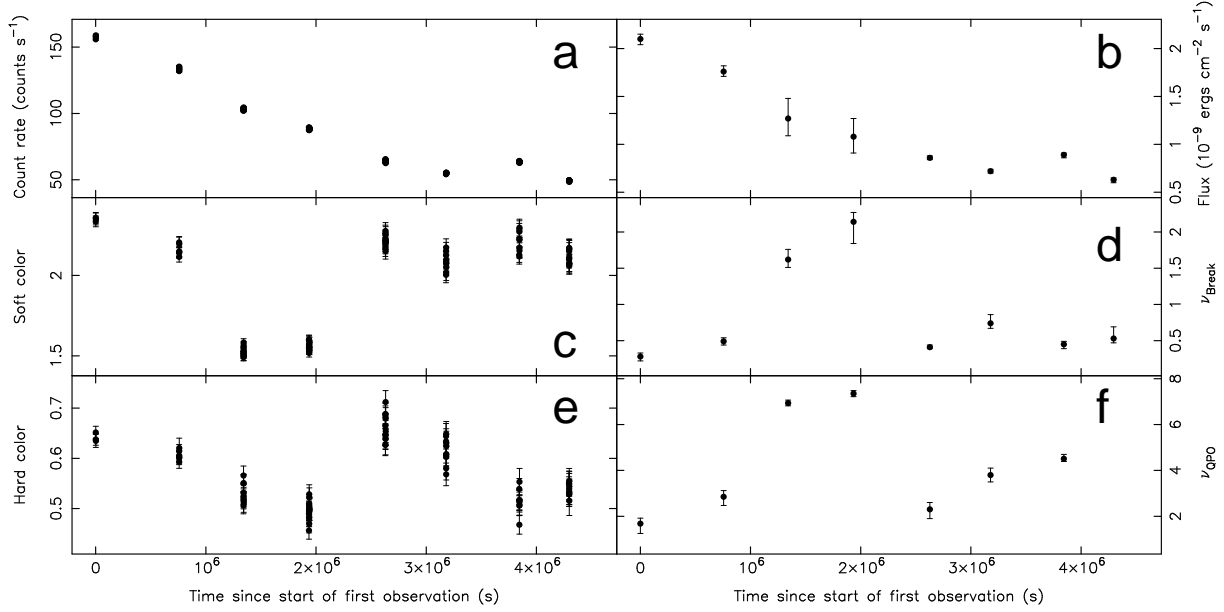


Fig. 1.— The 2.9–18.8 keV PCA count rate curve (*a*, PCU 2 only, the count rates are background subtracted), the 3.0–20.0 keV unabsorbed flux (*b*), the soft color (*c*, the count rate ratio between 4.1–7.5 keV and 2.9–4.1 keV), the break-frequency (*d*), the hard color (*e*, the count rate ratio between 11.4–18.8 keV and 7.5–11.4 keV), and the QPO frequency (*f*) as a function of time since the start of the first observation (60407-01-01-00; 2001 March 18). The bin size in *a*, *c*, and *e* is 256 seconds, to show that the variability in those quantities during each observation is less than the variability between observations. For the other panels, the whole data through out the separate observations was used (see Tab. 1 for the total time of each observation), to increase sensitivity.

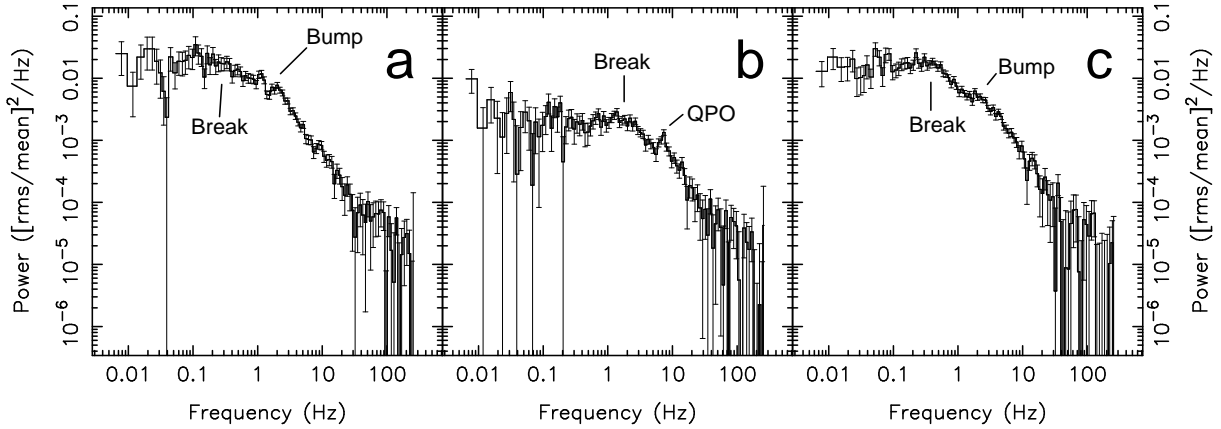


Fig. 2.— Power-spectra of the observations 60407-01-01-00 (a), 60407-01-04-00 (b), and 60407-01-05-00 (c). The Poisson level has been subtracted.

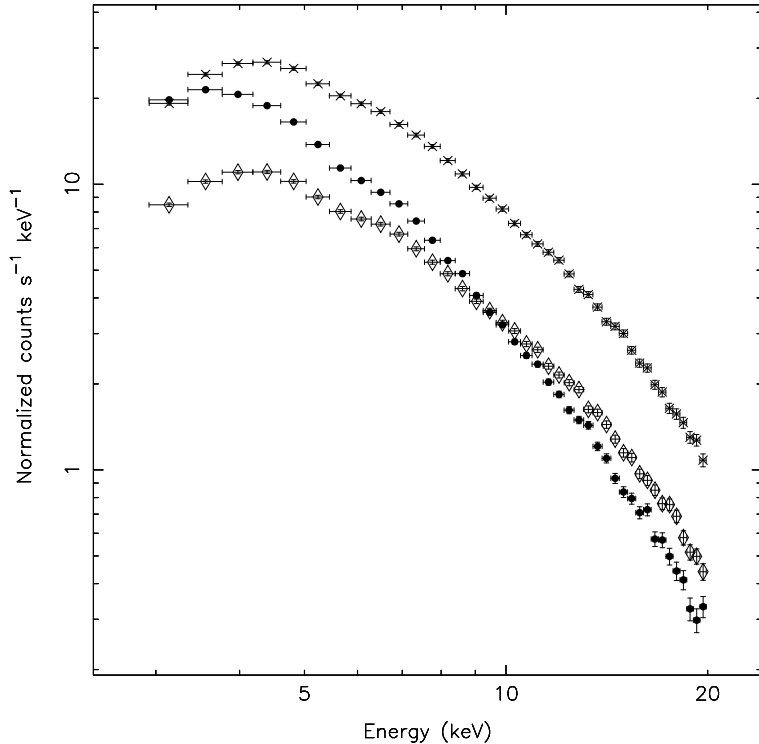


Fig. 3.— Energy spectra of the observations 60407-01-01-00 (crosses), 60407-01-04-00 (bullets), and 60407-01-05-00 (diamonds).

Table 1. Rapid X-ray variability and spectral parameters of each observation

Observation (60407-01-)	01-00	02-00	03-00	04-00	05-00	06-00	07-00	08-00
Obs. time (2001 UT)	March 18 05:42–06:20	March 26–27 23:56–00:32	April 2 18:22–19:09	April 9 15:25–17:14	April 17 15:41–17:43	April 24 00:51–01:53	May 1 17:35–18:55	May 6–7 23:04–00:02
Good time (ksec)	1.5	1.4	2.5	3.7	3.4	2.6	2.3	2.5
PCUs on	All	0,2,3 ^a	0,2,4	All ^a	All	0,2,3	0,2,4	0,2,3
Count rate ^b (cts s ⁻¹)	156	134	103	89	64	55	64	49
Power-spectrum fit parameters ^c								
Broken power-law								
Rms ^d (%)	18_{-2}^{+1}	15 ± 2	13 ± 1	13.6 ± 0.5	16.7 ± 0.5	18_{-2}^{+1}	13 ± 1	12 ± 1
ν_{break} (Hz)	0.28 ± 0.06	0.49 ± 0.05	1.6 ± 0.1	$2.1_{-0.3}^{+0.1}$	0.41 ± 0.03	0.7 ± 0.1	0.45 ± 0.06	$0.5_{-0.1}^{+0.2}$
Γ_1^e	$-0.4_{-0.2}^{+0.1}$	-0.4 ± 0.1	-0.29 ± 0.09	-0.04 ± 0.05	-0.10 ± 0.06	0.02 ± 0.07	-0.6_{-3}^{+2}	$-1.6_{-1.7}^{+0.9}$
Γ_2^e	1.05 ± 0.05	$1.2_{-0.1}^{+0.2}$	$1.4_{-0.1}^{+0.3}$	1.11 ± 0.08	1.2	$1.2_{-0.1}^{+0.2}$	1.2 ± 0.1	1.0 ± 0.1
QPO								
Rms ^d (%)	14_{-2}^{+3}	12_{-2}^{+3}	$5.4_{-0.7}^{+1.2}$ 6_{-1}^{+3}	4.2 ± 0.5	14 ± 1	8_{-1}^{+2}	$5.0_{-0.8}^{+1.0}$	<7
FWHM (Hz)	$2.9_{-0.5}^{+0.6}$	4 ± 1	$1.4_{-0.5}^{+0.9}$ 4_{-2}^{+5}	$1.4_{-0.3}^{+0.5}$	5.6 ± 0.7	2 ± 1	$0.8_{-0.5}^{+0.4}$	–
ν_{QPO}	$1.7_{-0.4}^{+0.2}$	$2.9_{-0.4}^{+0.3}$	6.9 ± 0.1	7.4 ± 0.1	$2.3_{-0.4}^{+0.3}$	3.8 ± 0.3	$4.5_{-0.1}^{+0.2}$	–
χ^2/dof	112/92	78/92	88/89	82/92	87/92	81/92	69/92	94/95
Energy-spectrum fit parameters ^f								
Power-law								
Index	1.87 ± 0.01	2.04 ± 0.02	2.12 ± 0.07	2.36 ± 0.06	1.89 ± 0.02	2.06 ± 0.02	2.33 ± 0.02	2.16 ± 0.02
Normalization	0.51 ± 0.02	0.60 ± 0.02	0.38 ± 0.06	0.6 ± 0.1	0.22 ± 0.01	0.25 ± 0.01	0.55 ± 0.02	0.27 ± 0.01
Flux ^g	1.93 ± 0.06	1.62 ± 0.05	0.9 ± 0.1	0.84 ± 0.14	0.80 ± 0.02	0.66 ± 0.02	0.75 ± 0.03	0.57 ± 0.03
MCD black-body								
T (keV)	–	–	0.86 ± 0.04	0.78 ± 0.06	–	–	–	–
Normalization	–	–	120 ± 30	108 ± 50	–	–	–	–
Flux ^g	–	–	0.24 ± 0.06	0.11 ± 0.05	–	–	–	–
Total flux ^g	2.10 ± 0.06	1.76 ± 0.06	1.3 ± 0.2	1.1 ± 0.2	0.86 ± 0.02	0.72 ± 0.02	0.89 ± 0.03	0.63 ± 0.03
χ^2_{red}	1.69	1.09	0.86	0.96	1.18	0.73	1.20	1.02

^aFor 02-00, PCU 0 and 2 were always on but PCU 3 only for 0.65 ksec. For 04-00, all detectors were on for the first 3.5 ksec, but only PCU 0 and 2 were on during the remaining 0.2 ksec.

^bThe count rates are for PCU 2 only and for 2.9–18.8 keV. The count rates are background subtracted.

^cAll errors are determined using $\Delta\chi^2 = 1$ and the upper limits are for 95% confidence levels

^dThe rms amplitudes are for the full 2–60 keV energy range of the *RXTE/PCA*.

^e Γ_1 is the slope of the power spectra for frequencies lower than ν_{break} and Γ_2 for frequencies higher than that. Γ_2 was fixed 1.2 (the averaged of the observations) for observation 5 because it could not be constrained during the fit.

^fThe column density was fixed to 1.4×10^{22} cm⁻² (except for observation 7, see text). The errors are for 90% confidence levels.

^gThe fluxes are for 3.0–20.0 keV and in units of 10^{-9} erg cm⁻² s⁻¹. The power-law and MCD fluxes are absorbed but the total flux is unabsorbed.